

Optical Modulation of Waveguiding in Spiropyran-Functionalized Polydiacetylene Microtube

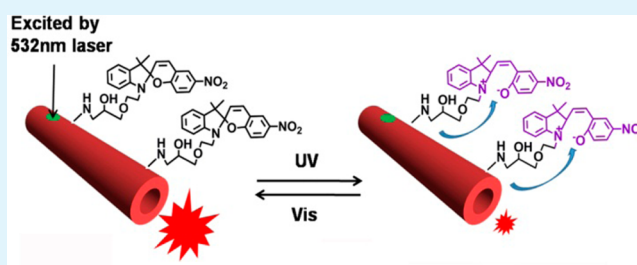
Hongyan Xia,^{†,‡} Yikai Chen,^{†,§} Guang Yang,[‡] Gang Zou,^{‡,*} Qijin Zhang,[‡] Douguo Zhang,^{*,§} Pei Wang,[§] and Hai Ming[§]

[‡]CAS Key Laboratory of Soft Matter Chemistry, Department of Polymer Science and Engineering, Key Laboratory of Optoelectronic Science and Technology in Anhui Province, and [§]Department of Optics and Optical Engineering, University of Science and Technology of China, Hefei, Anhui 230026, P. R. China

Supporting Information

ABSTRACT: Optical modulation of waveguiding and logic operations play significant roles in highly integrated optical communication components, optical computing, and photonic circuits. Herein, we designed and synthesized spiropyran-functionalized polydiacetylene (SFPDA) microtubes, and realized reversible optical modulation of waveguiding in SFPDA microtubes through fluorescence resonance energy transfer (FRET) between the PDA matrix and spiropyran in open merocyanine (MC) form within the surface of the microtubes. Because of the reversible isomerization characteristics of spiropyran units, we have realized resettable, multireadout logic system that includes OR and INHIBIT logic operations in SFPDA microtube.

KEYWORDS: polydiacetylene microtube, waveguide, spiropyran, optical modulation, logic gate operation



1. INTRODUCTION

Recently, extensive studies have been carried out on the development of materials and nano/microstructures to fabricate miniaturized optoelectronic devices.¹ A class of one-dimensional (1D) nano- and micro-sized materials including wires,² tubes,³ rods,⁴ and belts⁵ have been investigated for their potential applications in the field of photonic devices and sensing.^{6,7} Among them, 1D nano- and microstructures based on conjugated polymers materials possess excellent processing properties and chemically tunable optoelectronic characteristics and can be effective elements in the field of photonic circuits and sensing.^{8,9} Redmond et al.¹⁰ reported that 1D poly(9,9-dioctylfluorene) nanowires behaved as active optical waveguides to transport light efficiently. Fasano et al.¹¹ fabricated a conjugated polymer (PFO-PBAB) nanofiber waveguide by electrospinning, and the loss coefficients was as low as 100 cm⁻¹. Liu et al.¹² and Meng et al.¹³ fabricated polymer nanofiber waveguide incorporating quantum dots by electrospinning. In our previous work, 1D polydiacetylene (PDA) microtube have been successfully fabricated as an active optical waveguide.¹⁴ Compared to 1D organic photonic device based on the conjugated polymer nanowire or semiconductor quantum dot (QD)-incorporated polymer nanofibers, the novel PDA microtube waveguide system possesses several significant features. First, the high surface-to-volume ratios in the 1D microtube structure would facilitate the diffusion of the analyst molecules, leading to instant waveguiding modulation, which would facilitate the potential application in the field of smart materials and sensing. Second, the chemical properties

within the surface of PDA microtube can be effectively tailored through simple surface modification. Therefore, the waveguiding properties of PDA microtube can be modification with various functional units. Last, single PDA microtube waveguide system can be further integrated into the chips, which promise new opportunities in smart optical communications and integrated optoelectronic devices.

Although there are extensive studies focusing on the waveguiding properties of 1D active polymer materials, the flow of light in above 1D conjugated polymer nanofibers or microtube is predetermined and cannot be readily reversibly modulated during operation, limiting their practical application in optical communications and integrated optoelectronic devices. Therefore, it remains challenging to develop novel 1D conjugated polymer waveguide with tunable waveguide performance. Most of the present optical modulation have relied on two-photon absorption, the Kerr effect or nonlinear optical effects, which require a laser with extremely high power to achieve optical modulation.^{15,16} Great emphasis has been placed on optimizing the inorganic and organic microstructures of optical circuits based on complicated metallic nanostructures or evanescent wave mechanism¹⁷ to achieve optical modulation for future information technology. However, optical modulation of waveguiding in 1D conjugated polymer microtube based on the fluorescence resonance energy transfer (FRET)

Received: June 24, 2014

Accepted: August 14, 2014

Published: August 14, 2014

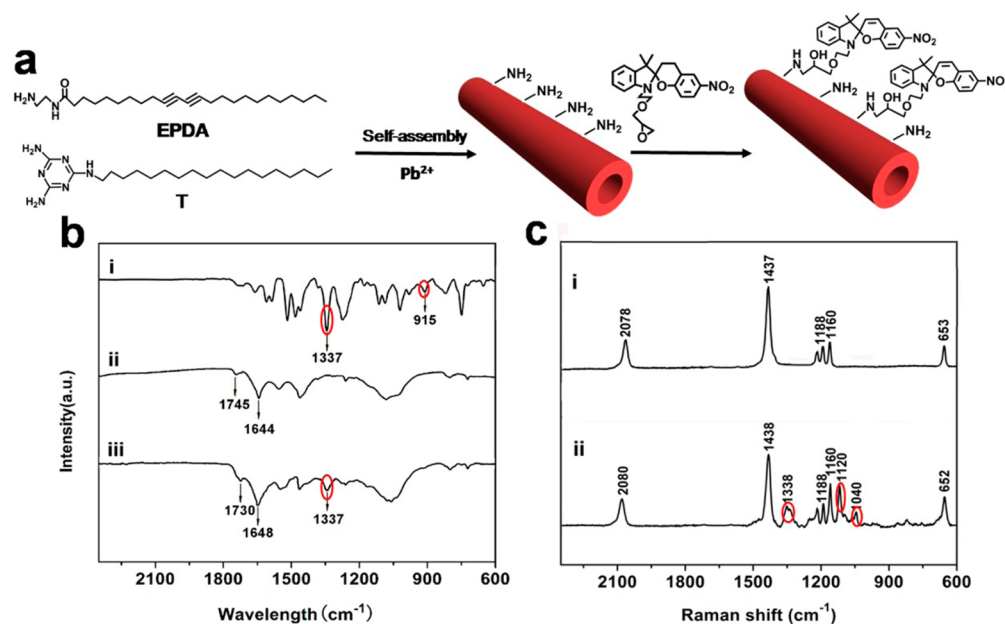


Figure 1. (a) Preparation of SFPDA microtubes. (b) FT-IR characterization of (i) epoxy-substituted spiro-6-nitrobenzopyryran, (ii) pure PDA microtubes, and (iii) SFPDA microtubes. (c) Raman spectrum of (i) pure PDA microtubes and (ii) SFPDA microtubes.

mechanism have seldom been reported. Herein, we design and synthesize spiro-6-nitrobenzopyryran-functionalized PDA (SFPDA) microtubes and attempted to realize reversible optical modulation of waveguiding in PDA microtube based on FRET between PDA matrix and the spiro-6-nitrobenzopyryran at the interface.

A lot of studies have been focus on spiro-6-nitrobenzopyryran derivatives which are developed as promising photochromes in application to functional materials such as optical switches, memory, and sensors.^{18,19} Spiro-6-nitrobenzopyryran is sensitive to surrounding media, displaying reversible structural transformation between colorless SP (spiro form), colorless MCH (protonated merocyanine form), and purple MC (merocyanine form) under thermal, pH, or light stimuli.²⁰ The absorption band of spiro-6-nitrobenzopyryran in MC form overlaps with the PL spectra of PDA; however, the absorption band of spiro-6-nitrobenzopyryran in SP form and MCH form do not.²¹ Thus, isomerization of spiro-6-nitrobenzopyryran between the MC and SP or MCH forms can be used to modulate the waveguiding properties of 1D SFPDA microtubes.

Further, optical logic gates have potential in ultrafast information processing and optical computing systems because they can fulfill various logic function operations.²² Great emphasis has been placed on optimizing the inorganic and organic microstructures of optical circuits based on silver nanowires to achieve optical logic operations for future information technology.²³ However, resettable optical logic operations in 1D conjugated polymers waveguides structure have not been achieved to date. In this paper, either the “ON” or “OFF” state of the out-coupled light from a PDA microtube waveguide can be achieved based on various combinational input signals, functioning as a basic optical Boolean logic unit. It is the first time that the photoresponsive SFPDA microtube with tunable optical modulation of waveguiding and optical logic operations have been realized through fluorescence resonance energy transfer (FRET) between the PDA matrix and open merocyanine (MC) form of spiro-6-nitrobenzopyryran within the surface of the microtubes. This responsive SFPDA microtube material may have potential application in ultrafast information processing, photonic circuits, and optical computing.

2. EXPERIMENTAL SECTION

2.1. Materials. 10,12-Pentacosadiynoic acid (DA; Tokyo Chemical Industry Co., Ltd.) was purified before use by dissolution in cyclopentanone and subsequent filtration. 1-(2-Hydroxyethyl)-3,3-dimethylindoline-6'-nitrobenzopyrylospiran (Tokyo Chemical Industry Co., Ltd.) A hand-held UV lamp ($\lambda = 254$ nm), hung 5 cm above the microtube, was used for structural transformation of spiro-6-nitrobenzopyryran units from SP to MC form. The light intensity of UV irradiation was about 15 mW cm^{-2} . Visible light irradiation experiments were performed by exposing the microtubes to a Xe lamp (with 435 interface filters, $\Delta\lambda = 5$ nm). The light intensity of visible light irradiation was about 20 mW cm^{-2} .

2.2. Preparation of SFPDA Microtubes. Ethylenediamine-substituted Pentacosadiacetylene (EPDA) and 2,4-diamino-6-octadecyl amino-1,3,5-triazine (T) (with molar ratio of EPDA:T = 9:1) were used to fabricate pure PDA microtube by hierarchical self-assembly procedure, similar as that in the reference.¹⁴ Upon thermal treatment, PDA microtubes transferred to “red-phase”, and exhibited strong fluorescence. Then the 200 μL of epoxy-substituted spiro-6-nitrobenzopyryran ethanol solution (3 mmol) was added to the above pure PDA microtube aqueous suspension solution and the mixture was stirred and stored in an incubator at room temperature for 10 h to ensure the reaction complete. Finally, the resulting SFPDA microtube was rinsed with deionized water several times in order to remove unreacted epoxy-substituted spiro-6-nitrobenzopyryran and other impurities.

2.3. Characterization. ^1H NMR spectra and FTIR experiments were carried out with a JEOL FX-90Q NMR 400 spectrometer and a MAGNA 750 FT-IR spectrometer at room temperature, respectively. Scanning electron microscopy (SEM) and Transmission electron microscopy (TEM) characterization were performed on a FEI Sirion200 system and a JEOL-2000 microscope (operated at 200 kV), respectively. The ultraviolet–visible (UV–vis) and Fluorescence spectra experiments were performed on a SHIMADZU UV-2550 PC spectrophotometer and a JY-ihR 550 spectrophotometer, respectively. Optical microscopy images and Confocal laser scanning microscopy (CLSM) images were obtained in BX-S1 fluorescence microscope and Olympus, FV 300, respectively. X-ray photoelectron spectroscopy (XPS) was characterized by using a VG ESCALAB MK-II photoelectron spectrometer. The Raman spectra were performed on a LABRAM-HR Confocal Laser MicroRaman Spectrometer with 514.5 nm radiation at room temperature.

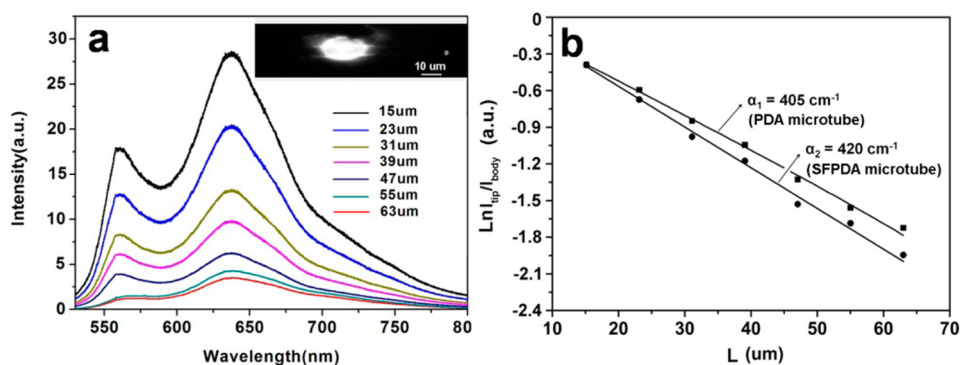


Figure 2. (a) Tip emission spectra of SFPDA microtube at different propagation distances (FL microscope image of SFPDA is shown as inset). (b) Logarithmic plots of relative PL intensities of pure PDA and SFPDA microtubes against propagation distance.

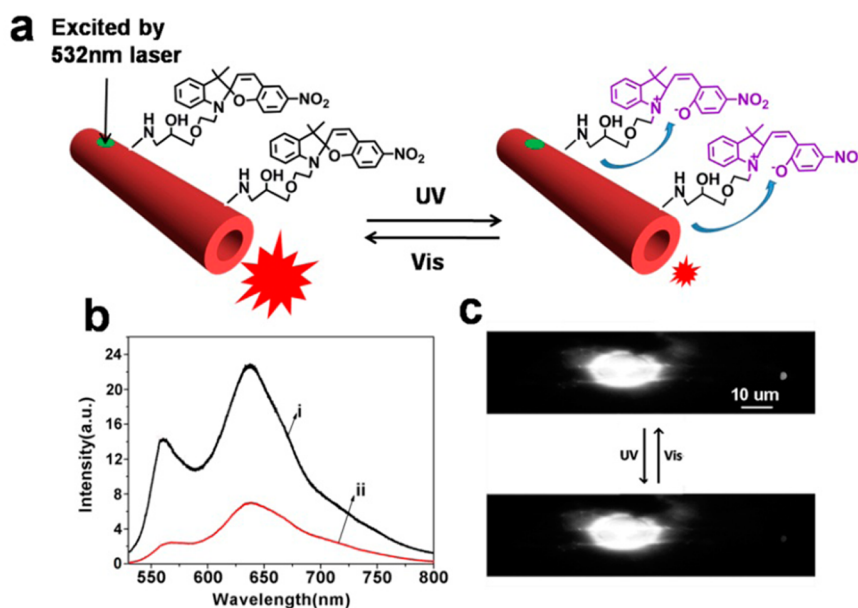


Figure 3. (a) Modulation of waveguiding in an SFPDA microtube. (b) Tip emission spectra of an SFPDA microtube (i) before and (ii) after UV light irradiation. (c) FL microscope images collected upon excitation of the same SFPDA microtube following UV and visible light irradiation.

3. RESULTS AND DISCUSSION

3.1. Characterization of the SFPDA Microtube. EPDA, T and epoxy-substituted spiropyran were synthesized according to reported procedures.^{24,25} The synthetic route, molecular structures and corresponding ¹H NMR spectra for epoxy-substituted spiropyran are shown in Figure S1 in the Supporting Information. Pure PDA microtube was prepared through similar procedure in ref 14. SEM characterization confirmed that PDA microtube have been successfully fabricated (see Figure S2 in the Supporting Information). Upon thermal treatment, PDA microtube transferred to “red-phase”, and emitted red fluorescent (see Figure S3a in the Supporting Information). The laser scanning confocal microscope (LSCM) characterization revealed the PDA microtube with hollow tubular microstructure (see Figure S3b in the Supporting Information). Then the SFPDA microtube was prepared by incubating above pure PDA microtube in epoxy-substituted spiropyran solution, since the epoxy group has a great tendency to react with the basic amino group in the surface of PDA microtube. The whole preparation process was schematically illustrated in Figure 1a. The characteristic bands of the triazine at 1644 and 1745 cm^{-1} were obtained. Upon

incubation with epoxy-substituted spiropyran, a new band (for the C–N stretching vibration) emerged at 1337 cm^{-1} , whereas the characteristic stretching bands of epoxy group at 913–916 cm^{-1} disappeared (Figure 1b), indicating the successful surface modification of PDA microtube with the spiropyran units. Moreover, the Raman spectrum of the functionalized PDA microtube consists of characteristic bands at 1437 and 2078 cm^{-1} , which should be attributed to the C=C and C≡C stretching vibrations of PDA backbone. And the Raman bands at 1338, 1120, and 1040 cm^{-1} (Figure 1c) were attributed to the indoline and chromene moieties in the SP form of spiropyran,²⁶ confirming the anchoring of the spiropyran group onto the surface of PDA microtube. All demonstrated that the SFPDA microtube have been prepared by the chemical reaction of epoxy group with the basic amino group in the surface of PDA microtube.

The optical waveguiding of a SFPDA microtube was studied by single-tube photoluminescence (PL) imaging (see Figure S4 in the Supporting Information). The tip of the SFPDA microtube exhibited bright PL, however, comparatively weaker emission could be observed for the body of the microtube. Because light was waveguided within the microtube through the intrinsic PL of “red-phase” PDA, the SFPDA microtube is

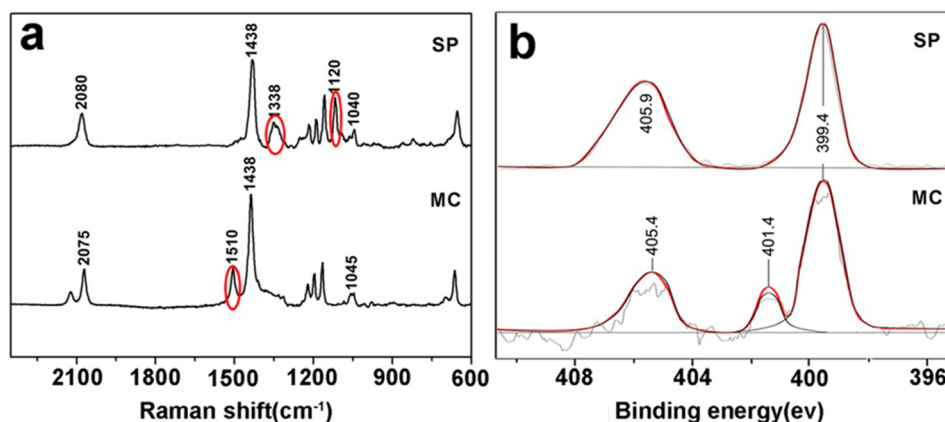


Figure 4. (a) Raman spectra of an SFPDA microtube before and after UV irradiation. (b) N 1s spectra of an SFPDA microtube before and after UV irradiation.

classified as an active waveguide. The tip emission intensity decreased almost exponentially with increasing of propagation length (Figure 2). The loss coefficient α is calculated to be 420 cm^{-1} ($\pm 10\%$), comparable to that of a pure PDA microtube (405 cm^{-1}).¹⁴ The propagation loss for the SFPDA microtube is $0.20 \text{ dB } \mu\text{m}^{-1}$, confirming that the spiropyran groups on the surface of the PDA microtube hardly affect its waveguiding properties (pure PDA microtube, $0.18 \text{ dB } \mu\text{m}^{-1}$). The waveguiding performance of SFPDA microtube is similar as that of pure PDA sample, and the dominant optical loss mechanism should be mainly ascribed to the reabsorption and light scattering arising from the fluctuation in internal materials density and surface roughness.¹⁴

3.2. Reversible Optical Modulation of Waveguiding in SFPDA Microtube. After 5 min UV irradiation (254 nm), the absorption band centered at 545 nm for the SFPDA microtubes obviously enhanced, which should be ascribed to the structural transformation of spiropyran units from SP to MC form. The PL intensity of SFPDA microtubes dramatically decreased (as show in Figure S5c, d in the Supporting Information). No obvious changes in the absorption or PL spectra could be observed for the bare PDA microtube during above process. The absorption band of spiropyran in MC form overlaps with the PL spectra of PDA; however, the absorption band of spiropyran in SP form does not.²¹ Thus, the efficient fluorescence quenching of SFPDA microtube upon UV irradiation should be assigned to the FRET between PDA microtube and the MC form of spiropyran units. It was anticipated that the isomerization of spiropyran between the MC and SP forms could be used to modulate the optical waveguiding properties of SFPDA microtube. After UV irradiation, the tip emission of the SFPDA microtube decreased significantly, however, the power of the incident excitation light and propagation distance from excitation spot to tip remained constant (Figure 3a). The propagation loss was about $0.29 \text{ dB } \mu\text{m}^{-1}$, much lower than that of the microtube before UV irradiation. Spatially resolved tip emission spectra are presented in Figure 3b. After UV irradiation, the tip emission spectrum of the SFPDA microtube exhibited greater relative quenching of the peak at around 567 nm, revealing that efficient quenching of SFPDA microtube should be mainly ascribed to the FRET mechanism between the MC form of spiropyran and PDA materials. After 20 min visible light irradiation (435 nm), the spiropyran units on the surface of the microtube transformed to the SP form, and the tip emission intensity and spectrum for

the SFPDA microtube returned to original values (Figure 3c). The modulation of the tip emission from the SFPDA microtube had an on/off ratio of approximately 3.2. Similar fluorometric changes at the tip of the microtube could be observed after two more regeneration and modulation cycles (see Figure S6 in the Supporting Information). These results clearly indicate that the fluorescence and waveguiding properties of the SFPDA microtube can be reversibly modulated by 254 and 435 nm light irradiation.

To confirm these findings, SFPDA microtubes before and after UV irradiation were examined by Raman spectroscopy and XPS. As presented in Figure 4a, the Raman spectrum of the SFPDA microtubes before UV irradiation contains bands at 1338 , 1120 , and 1040 cm^{-1} were ascribed to the indoline and chromene moieties in the SP form of spiropyran.²³ Upon UV irradiation for 5 min, the spiropyran units on the surface of the SFPDA microtubes transformed to the MC form, decreasing the intensity of the bands at 1338 and 1120 cm^{-1} and causing a new band to appear at 1510 cm^{-1} . The XPS results (Figure 4b) are consistent with the Raman spectra. Before UV irradiation, the N 1s core level region contained two peaks from the nitro group and indoline nitrogen at 405.9 and 399.4 eV, respectively. After UV irradiation, a new component was observed at 401.4 eV, indicating that the nitrogen was in the N^+ oxidation state, with accompanying decrease in intensity of the main indoline nitrogen peak.²⁷ The Raman and XPS results confirm that the optical modulation of waveguiding in SFPDA microtubes is directly related to the isomerization of the spiropyran units on their surface instead of the PDA matrix itself.

3.3. Optical Logic Operations in SFPDA Microtube. An important challenge in optical processing technology is the realization of logic operations. The spiropyran group displays reversible structural transformation between colorless SP, MCH and purple MC forms upon thermal, pH or light stimuli because the photophysical properties of spiropyran are sensitive to surrounding media.¹⁷ Therefore, the isomerization of spiropyran on the surface of the SFPDA microtubes could be used to modulate their tip emission (as shown in Figure S7 in the Supporting Information). On the basis of the above results, various logic gate operations could be realized. pH stimuli, UV and visible light irradiation were utilized as the input signals, and the tip emission of SFPDA microtube was taken as the output signal. We defined the SFPDA microtube with spiropyran in MC form as the initial state. In this case, the

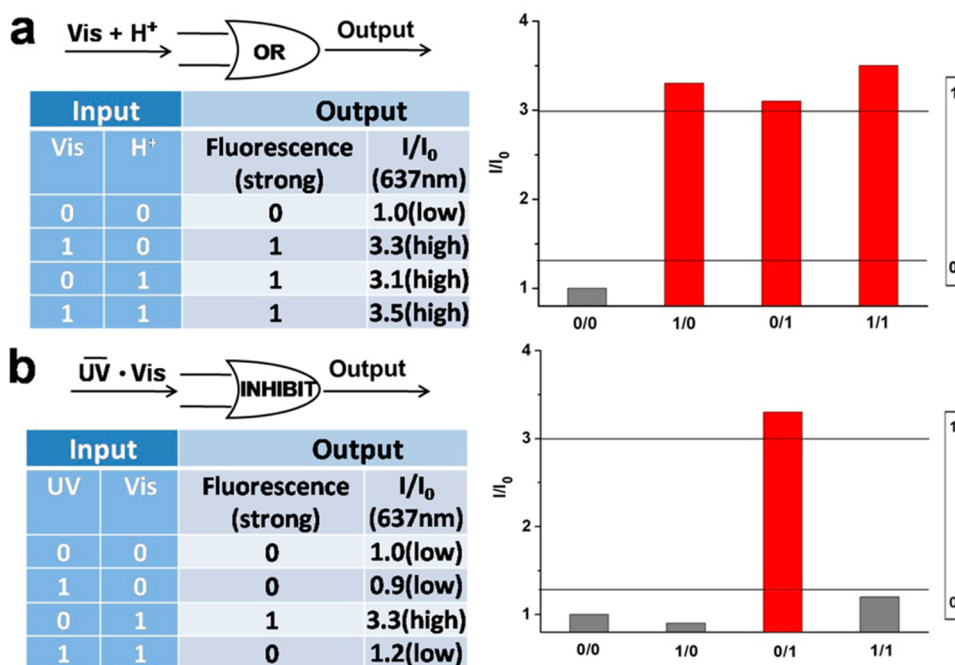


Figure 5. (a) Schematic illustration of an OR logic gate and the change of tip emission of the SFPDA microtube. (b) Schematic illustration of an INHIBIT logic gate and the change of tip emission of the SFPDA microtube.

tip emission from the SFPDA microtube is weak, which we exploited to design an OR logic gate. We employed irradiation at 435 nm and exposure to HCl gas as inputs, the presence and absence of them were defined as “1” and “0”, respectively. For outputs, we defined strong tip emission as “1” and weak as “0”. In the initial state (input 0/0), the tip emission was weak, and the output signal was “0”. With either visible light irradiation or exposure to HCl gas (input, 1/0 or 0/1), strong tip emission was detected (output = 1). Upon treatment with visible light and HCl gas (input, 1/1), similar strong tip emission could be detected (output = 1) (see Figure S8 in the Supporting Information). The spiropyran units transformed from MC to SP form upon 435 nm irradiation, or MCH form following exposure to HCl gas. In this case, the absorption band of colorless spiropyran units in SP form or MCH form did not overlap with the PL spectra of PDA, and no FRET between PDA and spiropyran occurred. Therefore, a higher I/I_0 was obtained for the presence of either or both inputs (1/0, 0/1, and 1/1) compared with 0/0 (Figure 5a).

An INHIBIT logic gate could be realized through similar FRET mechanism. We defined 435 or 254 nm light irradiation as “1”, whereas their absence was “0”. The strong and weak tip emission were defined as “1” and “0”, respectively. Before irradiation (input, 0/0), the tip emission of the SFPDA microtube was weak, and the output signal was “0”. After 5 min UV irradiation (input, 1/0), the spiropyran units remained in the MC form, and the tip emission was weak (output = 0). In the presence of both inputs (1/1), the tip emission was still weak, because the MC form of spiropyran units is more stable than the SP form under UV radiation. Upon 435 nm light irradiation alone (input, 0/1), the MC form of spiropyran transform to SP form, and no FRET between the PDA microtube and spiropyran occurred. In this case, tip emission of the microtube was enhanced greatly (output = 1) (see Figure S9 in the Supporting Information). A higher I/I_0 was obtained under 435 nm light alone (0/1) than for the three other states

(0/0, 1/0, 1/1) (Figure 5b). The reversibility of these spiropyran transformations means that the above logic gates operations can be easily reset through UV irradiation.

4. CONCLUSIONS

In summary, we fabricated SFPDA microtubes through chemical modification and realized reversible optical modulation of waveguiding through FRET between PDA matrix and spiropyran units in MC form within the surface of PDA microtube. Moreover, resettable, multireadout OR and INHIBIT logic operations in SFPDA microtube have been achieved. Because the surface of PDA microtube can be effectively tailored through simple surface modification with other environmental response elements, reversible modulation of waveguiding performance in PDA microtube and optical logic operation upon external stimuli (e.g., electrical stimuli, biological stimuli) can be achieved through similar FRET mechanism. The controllable switching of guided light in a single SFPDA microtube and resettable logic gate operations may pave the way for rational design of smart conjugated-polymer photonic devices for future information technology.

■ ASSOCIATED CONTENT

Supporting Information

Synthetic route and ¹H NMR spectrum of epoxy-substituted spiropyran; SEM characterization of PDA microtube; Fluorescence microscopy image and LSCM image of PDA microtube upon thermal treatment; the experimental setup for the optical waveguide experiments; Scheme for the multistimuli-responsive modulation of waveguiding in the SFPDA microtube. This material is available free of charge via the Internet at <http://pubs.acs.org>.

■ AUTHOR INFORMATION

Corresponding Authors

*E-mail: ganzou@ustc.edu.cn.

*E-mail: dgzhang@ustc.edu.cn.

Author Contributions

[†]H.X. and Y.C. contributed equally to this work. The manuscript was written through contributions of all authors. All authors have given approval to the final version of the manuscript.

Notes

The authors declare no competing financial interest.

ACKNOWLEDGMENTS

This research was carried out with funding from the National Natural Science Foundation of China (51173176, 51273186, 21074123, 91027024, 11374286, and 61036005), the Chinese Academy of Sciences (kjcx2-yw-m11), the Fundamental Research Funds for the Central Universities (WK2060200012), and the National Key Basic Research Program of China (No. 2012CB921900, 2012CB922003, and 2013CBA01703).

REFERENCES

- (1) Yan, B. B.; Liao, L.; You, Y. M.; Xu, X. J.; Zheng, Z.; Shen, Z. X.; Ma, J.; Tong, L. M.; Yu, T. Single-Crystalline V₂O₅ Ultralong Nanoribbon Waveguides. *Adv. Mater.* **2009**, *21*, 2436–2440.
- (2) Kong, Q. H.; Liao, Q.; Xu, Z. Z.; Wang, X. D.; Yao, J. N.; Fu, H. B. Epitaxial Self-assembly of Binary Molecular Components into Branched Nanowire Heterostructures for Photonic Applications. *J. Am. Chem. Soc.* **2014**, *136*, 2382–2388.
- (3) Gaufres, E.; Izard, N.; Noury, A.; Roux, X. L.; Rasigade, G.; Beck, A.; Vivien, L. Light Emission in Silicon from Carbon Nanotubes. *ACS Nano* **2012**, *6*, 3813–3819.
- (4) Zhu, D. F.; He, Q.; Chen, Q. G.; Fu, Y. Y.; He, C.; Shi, L. Q.; Meng, X.; Deng, C. M.; Cao, H. M.; Cheng, J. G. Sensitivity Gains in Chemosensing by Optical and Structural Modulation of Ordered Assembly Arrays of ZnO Nanorods. *ACS Nano* **2011**, *5*, 4293–4299.
- (5) Liu, M.; Yin, X. B.; Ulin-Avila, E.; Geng, B.; Zentgraf, T.; Ju, L.; Wang, F.; Zhang, X. A Graphene-based Broadband Optical Modulator. *Nature* **2011**, *474*, 64–67.
- (6) Moon, H.; Zeis, R.; Borkent, E. J.; Besnard, C.; Lovinger, A. J.; Siegrist, T.; Kloc, C.; Bao, Z. N. Synthesis, Crystal Structure, and Transistor Performance of Tetracene Derivatives. *J. Am. Chem. Soc.* **2004**, *126*, 15322–15323.
- (7) Zhao, Y. S.; Fu, H. B.; Peng, A. D.; Ma, Y.; Liao, Q.; Yao, J. N. Construction and Optoelectronic Properties of Organic One-Dimensional Nanostructures. *Acc. Chem. Res.* **2010**, *43*, 409–418.
- (8) O'Carroll, D.; Lieberwirth, I.; Redmond, G. Melt-Processed Polyfluorene Nanowires as Active Waveguides. *Small* **2007**, *3*, 1178–1183.
- (9) Liao, Q.; Fu, H. B.; Yao, J. N. Waveguide Modulator by Energy Remote Relay from Binary Organic Crystalline Microtubes. *Adv. Mater.* **2009**, *21*, 4153–4157.
- (10) O'Carroll, D.; Lieberwirth, I.; Redmond, G. Melt-Processed Polyfluorene Nanowires as Active Waveguides. *Small* **2007**, *3*, 1178–1183.
- (11) Fasano, V.; Polini, A.; Morello, G.; Moffa, M.; Camposeo, A.; Pisignano, D. Bright Light Emission and Waveguiding in Conjugated Polymer Nanofibers Electrospun from Organic Salt Added Solutions. *Macromolecules* **2013**, *46*, 5935–5942.
- (12) Liu, H.; Edel, J. B.; Bellan, L. M.; Craighead, H. G. Electrospun Polymer Nanofibers as Subwavelength Optical Waveguides Incorporating Quantum Dots. *Small* **2006**, *2*, 495–499.
- (13) Meng, C.; Xiao, Y.; Wang, P.; Zhang, L.; Liu, Y. X.; Tong, L. M. Quantum-Dot-Doped Polymer Nanofibers for Optical Sensing. *Adv. Mater.* **2011**, *23*, 3770–3774.
- (14) Hu, W. L.; Chen, Y. K.; Jiang, H.; Li, J. G.; Zou, G.; Zhang, Q. J.; Zhang, D. G.; Wang, P.; Ming, H. Optical Waveguide Based on a Polarized Polydiacetylene Microtube. *Adv. Mater.* **2014**, *26*, 3136–3141.
- (15) Liang, T. K.; Nunes, L. R.; Tsuchiya, M.; Abedin, K. S.; Miyazaki, T.; Van Thourhout, D.; Bogaerts, W.; Dumon, P.; Baets, R.; Tsang, H. K. High Speed Logic Gate Using Two-photon Absorption in Silicon Waveguides. *Opt. Commun.* **2006**, *265*, 171–174.
- (16) Xu, Q.; Lipson, M. All-optical Logic Based on Silicon Micro-ring Resonators. *Opt. Express* **2007**, *15*, 924–929.
- (17) Soltani, M.; Lin, J.; Forties, R. A.; Iaman, J. T.; Saraf, S. N.; Flubright, R. M.; Lipson, M.; Wang, M. D. Nanophotonic Trapping for Precise Manipulation of Biomolecular Arrays. *Nat. Nanotechnol.* **2014**, *9*, 448–452.
- (18) Zaghoul, Y. A.; Zaghoul, A. R. M. Complete All-optical Processing Polarization Based Binary Logic Gates and Optical Processors. *Opt. Express* **2006**, *14*, 9879–9895.
- (19) Wei, H.; Wang, Z.; Tian, X.; Kall, M.; Xu, H. Cascaded Logic Gates in Nanophotonic Plasmon Networks. *Nat. Commun.* **2011**, *2*, 387–392.
- (20) Kameda, M.; Sumaru, K.; Kanamori, T.; Shinbo, T. Probing the Dielectric Environment Surrounding Poly(N-isopropylacrylamide) in Aqueous Solution with Covalently Attached Spirobenzopyran. *Langmuir* **2004**, *20*, 9315–9319.
- (21) Xia, H. Y.; Xu, Y. Y.; Yang, G.; Jiang, H.; Zou, G.; Zhang, Q. J. A Reversible Multi-Stimuli-Responsive Fluorescence Probe and the Design for Combinational Logic Gate Operations. *Macromol. Rapid Commun.* **2014**, *35*, 303–308.
- (22) Liu, D. B.; Chen, W. W.; Sun, K.; Deng, K.; Zhang, W.; Wang, Z.; Jiang, X. Y. Resettable, Multi-Readout Logic Gates Based on Controllably Reversible Aggregation of Gold Nanoparticles. *Angew. Chem., Int. Ed.* **2011**, *50*, 4103–4107.
- (23) Zhang, S. P.; Wei, H.; Bao, K.; Hakanson, U.; Halas, N. J.; Nordlander, P.; Xu, H. X. Chiral Surface Plasmon Polaritons on Metallic Nanowires. *Phys. Rev. Lett.* **2011**, *107*, 1–5.
- (24) Barberá, J.; Puig, L.; Romero, P.; Serrano, J. L.; Sierra, T. Propeller-like Hydrogen-Bonded Banana–Melamine Complexes Inducing Helical Supramolecular Organizations. *J. Am. Chem. Soc.* **2006**, *128*, 4487–4492.
- (25) Lee, J.; Jun, H.; Kim, J. Polydiacetylene–Liposome Microarrays for Selective and Sensitive Mercury(II) Detection. *Adv. Mater.* **2009**, *21*, 3674–3677.
- (26) Ivashenko, O.; Herpt, J. T. V.; Feringa, B. L.; Rudolf, P.; Browne, W. R. UV/Vis and NIR Light-Responsive Spiropyran Self-Assembled Monolayers. *Langmuir* **2013**, *29*, 4290–4297.
- (27) Ivashenko, O.; Herpt, J. T. V.; Feringa, B. L.; Rudolf, P.; Browne, W. R. Electrochemical Write and Read Functionality through Oxidative Dimerization of Spiropyran Self-Assembled Monolayers on Gold. *J. Phys. Chem. C* **2013**, *117*, 18567–18577.